Wearable salivary uric acid mouthguard biosensor with integrated wireless electronics

Jayoung Kim, Somayeh Imani, William R. de Araujo, Julian Warchall, Gabriela Valdés-Ramírez, Thiago R.L.C. Paixão, Patrick P. Mercier, Joseph Wang

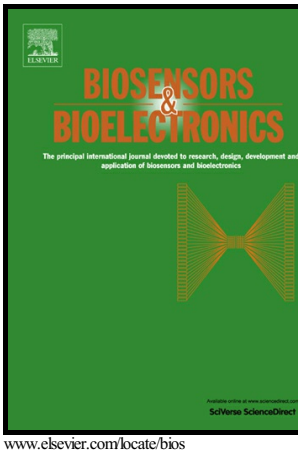

www.elsevier.com/locate/bios

PII: S0956-5663(15)30287-6
DOI: http://dx.doi.org/10.1016/j.bios.2015.07.039
Reference: BIOS7857

To appear in: *Biosensors and Bioelectronic*

Received date: 29 May 2015
Revised date: 16 July 2015
Accepted date: 17 July 2015

Cite this article as: Jayoung Kim, Somayeh Imani, William R. de Araujo, Julian Warchall, Gabriela Valdés-Ramírez, Thiago R.L.C. Paixão, Patrick P. Mercier and Joseph Wang, Wearable salivary uric acid mouthguard biosensor with integrated wireless electronics, *Biosensors and Bioelectronic* http://dx.doi.org/10.1016/j.bios.2015.07.039

Wearable salivary uric acid mouthguard biosensor with integrated wireless electronics

Jayoung Kim[a‡], Somayeh Imani[b‡], William R. de Araujo[a,c‡], Julian Warchall[b], Gabriela Valdés-Ramírez[a], Thiago R.L.C. Paixão[c], Patrick P. Mercier*[b], Joseph Wang*[a]

[a]Department of Nanoengineering, University of California, San Diego, La Jolla, California 92093, USA

*E-mail: josephwang@ucsd.edu

[b]Department of Electrical & Computer Engineering, University of California, San Diego, La Jolla, California 92093, USA

*E-mail: pmercier@ucsd.edu

[c]Instituto de Química -Universidade de São Paulo, Av Prof Lineu Prestes, 748, São Paulo, SP, 05508–000, Brazil

‡Authors contributed equally to this work

Highlights

- Integrated wireless mouthguard bio-sensor for real time human salivary uric acid monitoring.
- Includes Bluetooth 4.0 wireless link for data transmission.
- Salivary uric acid is electrochemically detected by prussian Blue/Uricase/glutarldehyde/poly-ortrophenylendiamine bio-sensing platform.
- Potential applications in wearable health-care monitoring.

Keywords: Wearable sensor; wireless electronics; salivary uric acid; mouthguard biosensor; screen printing

Abstract

This article demonstrates an instrumented mouthguard capable of non-invasively monitoring salivary uric acid (SUA) levels. The enzyme (uricase)-modified screen printed electrode system has been integrated onto a mouthguard platform along with anatomically-miniaturized instrumentation electronics featuring a potentiostat, microcontroller, and a Bluetooth Low Energy (BLE) transceiver. Unlike RFID-based biosensing systems, which require large proximal power sources, the developed platform enables real-time wireless transmission of the sensed information to standard

smartphones, laptops, and other consumer electronics for on-demand processing, diagnostics, or storage. The mouthguard biosensor system offers high sensitivity, selectivity, and stability towards uric acid detection in human saliva, covering the concentration ranges for both healthy people and hyperuricemia patients. The new wireless mouthguard biosensor system is able to monitor SUA level in real-time and continuous fashion, and can be readily expanded to an array of sensors for different analytes to enable an attractive wearable monitoring system for diverse health and fitness applications.

1. Introduction

Wearable sensors have been receiving considerable recent attention because of their great promise for on-body monitoring of a wide range of relevant parameters for health, fitness, and biomedicine applications (Ghafar-Zadeh et al., 2015; Andreu Perez et al., 2015; Soh et al., 2015; Corrie et al., 2015). While the majority of existing wearable technologies focus on monitoring physical parameters (e.g., motion, respiration rate, etc.) or electrophysiology (e.g., ECG, EMG, etc.), there is tremendous interest in developing wearable sensors for important chemical markers relevant to health or fitness (Windmiller and Wang, 2013; Matzeu et al., 2015; Bandodkar and Wang 2014). Significant progress has been made recently in developing wearable electrochemical sensors that detect metabolites and electrolytes in sweat, saliva, and tears (Jia et al., 2013; Bandodkar et al., 2013; Bandodkar et al., 2014b; Bandodkar et al., 2015; Kim et al., 2014; Kim et al., 2015; Zuliani et al., 2014; Thomas et al., 2012; Yao et al., 2012). Saliva is a great diagnostic fluid providing an alternative to direct blood analysis via the permeation of blood constituents without any skin-piercing for blood sampling. Early work in electrochemical salivary sensors was demonstrated by Graf in the 1960s, measuring pH and fluoride ion levels on a partial denture (Graf and Mühlemann 1966, 1969). Several efforts have more recently developed salivary sensors based on screen-printing techniques that take advantage of scalable low-cost fabrication. For example, Diamond's group has developed disposable potentiometric pH sensor strips (Zuliani et al., 2014), and our group has demonstrated a wearable salivary lactate sensor using a mouthguard platform (Kim et al., 2014).

Despite these recent advances, the realization of wearable biosensors for real-time monitoring of chemical markers is limited by the small number of demonstrated

target analytes and the lack of integrated wireless data transmission in measurement platforms. While it was predicted that the wireless wearable chemo-sensors for personal health/wellness was slated to expand rapidly (Diamond et al., 2008), challenges such as power consumption and size of wireless sensor systems remain. Mannoor et al reported a novel graphene-based wireless resistometric sensor for continuous monitoring of bacteria on a silk dental tattoo platform (Mannoor et al., 2014); however, this platform does not measure salivary metabolites and requires a large active device to be held in close proximity to the sensor, which is inconvenient for continuous real-time readout. In another work, a radio-frequency identification (RFID) wireless sensor tag with potentiometric input has been introduced (Kassal et al., 2013). The tag, which is too large for integration in typical anatomically-sized platforms, is powered by a 3 V battery, and a larger reader device still needs to be positioned in close proximity to the tag for successful data readout. A similar system has been recently developed by our group (Kassal et al. 2015) to implement a smart bandage, though the drawbacks of short-range communication and bulky monitoring devices remain.

The size of the wireless system can potentially be decreased by transitioning from near-field or RFID-like approaches, which require a large proximal reader device, to far-field radios that communicate with small receivers that can potentially be placed far away. Wireless monitoring of blood glucose and lactic acid level in fish has been reported by Endo et al. (2009) and Hibi et al. (2012), respectively. These designs utilized a 3102BP Pinnacle Technology wireless potentiostat operating at 916.5MHz, which transmits sensed data to a proprietary receiver (3100RX, Pinnacle Technology Inc.). On the other hand, more common communication links, such as Bluetooth, do not require specific reader/receiver designs; therefore, a broad range of receivers can be employed. For example, a Bluetooth-enabled system for real time monitoring of physical parameters was proposed by Depari et al. (2013). The system consists of a commercial Bluetooth earphone along with a PPG sensor, tissue impedance sensor, and interface circuits. In another work, a portable smart-phone based impedance TNT monitoring system has been reported (Zhang et al. 2015). These examples employed Bluetooth 2.0 and Hands-Free Profile (HFP) commercial based systems and have opportunities to reduce power consumption and size.

In this work, the wireless amperometric circuit, paired with a Bluetooth low energy (BLE) communication system-on-chip (SoC) for miniaturized and low-power

operation, is fully integrated into a novel salivary metabolite mouthguard biosensor for continuous and real-time amperometric monitoring. The mouthguard enzyme electrode is applied for the detection of uric acid (UA), which is the end product of purine metabolism in the human body. An abnormal concentration of UA is a biomarker for various diseases, including hyperuricemia, gout, lesch-Nyhan syndrome, and renal syndrome (Nyhan et al., 1997; Moran et al., 2003; Falasca et al., 2006; Nakagawa et al., 2006; Merriman et al., 2011;). In addition, higher UA levels implicate a higher future risk of type 2 diabetes and its severity and complications (Costa et al., 2002; Zloczower et al., 2007; Dehghan et al., 2008; Bhole et al., 2010). UA can also be an indicator of physical stress induced reactive oxygen species (ROS), acting as a free radical scavenger (Hellsten et al., 1997; Owen-smith et al., 1998). While blood UA (BUA) measurements require invasive blood collection, salivary uric acid (SUA) measurements could be carried out non-invasively and in a continuous real-time manner. Shibasaki et al. (2012) and Soukup et al. (2012) have found a good correlation of UA blood and saliva levels, demonstrating that this metabolite can be monitored in saliva in a non-invasive way without need for blood sampling.

The new mouthguard biosensor has been fabricated using a well-established screen-printing technology on a flexible PET (polyethylene terephthalate) substrate. Chemical modification of the printed working electrode Prussian-blue transducer has been made by crosslinking the uricase enzyme and electropolymerizing o-phenylenediamine. The performance of the new mouthguard biosensor has been evaluated through UA measurements in artificial saliva and undiluted human saliva. The feasibility of the new mouthguard biosensor system for clinical use has been tested by monitoring a hyperuricemia patient under medication treatment. Finally, the sensor has been integrated with a wireless amperometric circuitry to realize a comfortable wearable device (Fig. 1A). The resulting integrated mouthguard biosensor offered real-time uric-acid measurements along with wireless data transmission. A BLE chipset has been adopted to enable wireless connectivity to a smartwatch, smartphone, tablet, portable media player, laptop or any other BLE-enabled device. In the following sections, we will describe the design of the integrated mouthguard biosensor coupled with a miniaturized printed circuit board for wireless data collection and its attractive performance in the continuous monitoring of salivary UA.

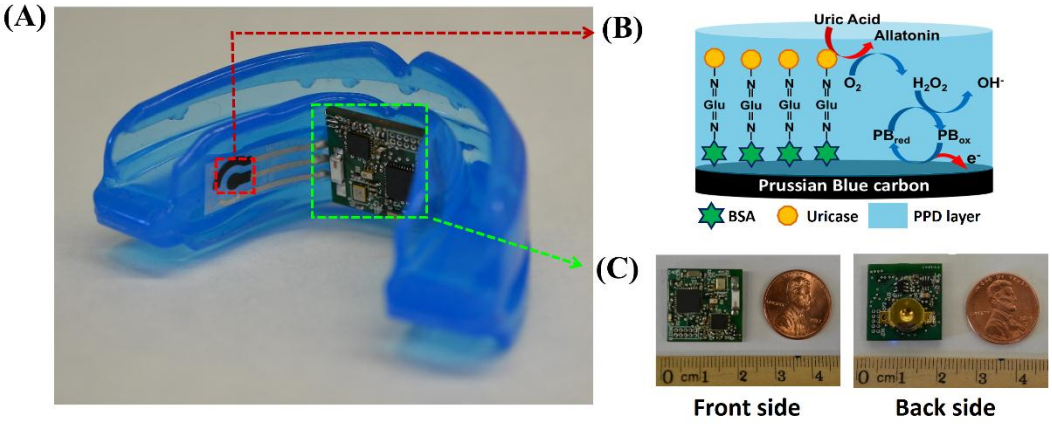

Fig. 1. (A) Photograph of the mouthguard biosensor integrated with wireless amperometric circuit board. (B) Reagent layer of the chemically modified printed Prussian-Blue carbon working electrode containing uricase for SUA biosensor. (C) Photograph of the wireless amperometric circuit board: front side (left) and back side (right).

2. Materials and methods

2.1. Chemicals and instruments

Uricase (5U/mg) from Candida sp., o-phenylenediamine (OPD), L-lactic acid (LA), D-glucose, L-ascorbic acid (AA), acetaminophen (ACT), uric acid (UA), sodium sulfate, sodium chloride, calcium chloride, potassium chloride, citric acid, potassium thiocyanate, ammonium chloride, potassium monobasic, potassium dibasic, bovine serum albumin (BSA), and glutaraldehyde solution were obtained from Sigma Aldrich (St. Louis, MO) and were used without further purification or modification. Ultrapure water (18.2 MΩ•cm) was employed in all of our experiments. Allopurinol® 150mg was obtained at a local pharmacy.

A MPM SPM semi-automatic screen printer (Speedline Technologies, Franklin, MA) was used for printing electrodes. The sensor patterns were designed using AutoCAD (Autodesk, San Rafael, CA) and stencils were patterned on 75 μm thick stainless steel stencils (Metal Etch Services, San Marcos, CA). A CH Instruments (Austin, TX) model 621A electrochemical analyzer was employed for the electrochemical characterization in Section 2.2-2.5.

2.2 Fabrication and chemical modification of mouthguard biosensor

Mouthguard biosensors were screen-printed on flexible PET substrate with three separate layers. First, an Ag/AgCl conductive ink (124-36, medical grade, Creative Materials Inc., MA USA) was printed to offer reference electrode as well as current collector for electrochemical measurement. Subsequently, Prussian-blue-graphite ink (C2070424P2, Gwent Inc., Torfaen, UK) was printed for working and counter electrodes. The third (insulator) layer was printed with Dupont 5036 dielectric paste (Wilmington, DE, USA) to define electrode area. After every printing step, the printed layers were cured at 80 °C for 20 min. The defined working electrode is in a circle shape with a 3 mm diameter. The working electrode is additionally modified with enzyme and anti-biofouling membranes. First, 3.0 mg of uricase were mixed with 2 mg of BSA and 1 µl of 8 % glutaraldehyde solution in 200 µl of potassium phosphate buffer. 3 µl of mixed solution were then drop-casted on the working electrode and dried for 30 minutes. Next, PPD (polymerized-OPD) was deposited on the enzyme layer by electropolymerization of OPD by applying 0.6 V (vs. Ag/AgCl) for 5 minutes in 0.1 M phosphate buffer (pH 7.0) solution containing 10 mM OPD, 5 mM sodium sulfate to minimize biofouling and interference effects from saliva constituents. Fig. 1B shows the chemical constitution of the modified working electrode on the mouthguard platform. The fabricated enzyme electrode was attached to the mouthguard and wired to connect either to the miniaturized printed circuit board for wireless data collection or to a lab-scale potentiostat.

2.3 Electrochemical evaluation in artificial saliva

The electrochemical performance of the salivary UA biosensor on mouthguard was first evaluated in artificial saliva, which has a similar electrolyte concentration to human saliva (Claver et al., 2009). The artificial saliva was prepared by dissolving 5 mM of NaCl, 1 mM of $CaCl_2$, 15 mM of KCl, 1 mM of citric acid, 1.1 mM of KSCN, and 4 mM of NH_4Cl in distilled water. The pH of artificial saliva was adjusted to 6.7, which is an average pH of healthy human saliva (Chicharro et al., 1998). Chronoamperometric measurements of UA at the PB-PPD-Uricase biosensor were carried out by stepping the potential to -0.3 V (vs. Ag/AgCl) for 60 seconds after 1minute of incubation in the sample solution. The calibration curve was obtained by chronoamperometric measurements with 50 µM increments of UA concentrations up

to 1 mM in 100 µl of artificial saliva. The stability of the biosensor was examined in a 350 µM UA solution at 10 minute intervals over a 2 hour long operation. The sensor was kept in artificial saliva between such successive measurements. Selectivity was evaluated in 350 µM UA in artificial saliva under stirring and fixed potential conditions in the presence of relevant physiological interferents: 200 µM AA, 800 µM glucose, 100 µM ACT, and 1000 µM LA. The concentration of each interferents was chosen under consideration of increment by intake of supplements, disease, and exercise based on its average level (Mäkilä et al., 1969; Abikshyeet et al., 2012; Chicharro et al., 1998; Smith et al., 1991).

2.4. Electrochemical evaluation in undiluted human saliva

Human saliva samples were collected from volunteers by using the "passive drool" method (Navazesh et al., 1993). The collected samples were directly used for electrochemical measurements without any treatment. The concentration of UA in the saliva samples was determined via the standard addition method by applying same experimental conditions used in artificial saliva (E_{APP}=-0.3 V for 60 seconds). Briefly, 100 µl of saliva droplet on the electrode surface was incubated for 60 seconds and measured by stepping the potential to -0.3 V for 60 seconds to obtain saliva baseline response. Subsequently, the saliva sample was spiked with the UA standard solution to give a 0.2 mM concentration, followed by 60 second incubation and 60 second for current measurement, repeating the process up to 1 mM uric acid. The concentration of uric acid in saliva sample was calculated as the intercept where the produced current is zero. For stability test in real saliva samples, signals were measured every 20 minutes and the sample was replaced at every measurement considering the flow rate of saliva in mouth (unstimulated: 1 ml/min, stimulated: 2 ml/min) (Humphrey et al., 2001). The sensor was immersed in saliva between such successive runs.

2.5. Monitoring SUA level of hyperuricemia patient under medication treatment

To help validate the utility of the developed sensor for monitoring health conditions, SUA levels were monitored in two types of volunteer: a hyperuricemia patient and a healthy volunteer. To verify fluctuations of SUA level during the day, saliva was collected and measured hourly without any additional treatment for a time period of 5 hours. Each sample was measured by a standard addition method to quantify the amount of UA in the saliva sample, as mentioned in section 2.4. When

the hyperuricemia patient had a higher SUA level than normal, Allopurinol®, (the medication used to treat hyperuricemia), was orally administered for 4 days. In each of these four days, saliva was collected at three separate times and the corresponding UA concentration was estimated via the standard addition method as described in section 2.4.

2.6. Design and fabrication of wireless amperometric printed circuit board

Unlike near-field communication (NFC) chipsets that can only communicate over a distance of a few centimeters, a Bluetooth Low Energy (BLE) chipset was adopted in this work to enable wireless connectivity to a smartwatch, smartphone, or laptop over the distance of several meters, enabling unobtrusive, real-time monitoring. Specifically, the design employed a Texas Instrument (TI) CC2541 BLE System-on-Chip for communication and processing. An LMP91000 Analog Front End (AFE), programmable through an I2C interface driven by the CC2541, was used as the on-board potentiostat. The fabricated printed circuit board assembly (PCBA), shown in Fig. 1C, measured 1.8 cmx1.9 cm. A Johanson Technology 2.45 GHz chip antena (2450AT42A100) and impedance matched balun (2450BM15A0002) were employed for wireless transmission. Two 396/397 watch batteries (2x1.55 V, 33 mAh each) in series were utilized as a power source, regulated for the electronics via a TPS61220 boost converter and an LM4120 low-dropout voltage regulator. The board consumed, on average, 7 mA from a 3 V supply during "active mode" (21 mW). In order to maximize the battery life, a 0.6 mW "sleep mode" was engaged during extended periods of time when measurements were not being taken. In this mode, the LMP91000 entered a "deep sleep" state while the CC2541 was placed in power mode 1 (with a 4 μs wake-up time). A third mode, "stand-by," was used when there was a moderate delay between data transmissions. In this mode, the LMP91000 remained in the potentiostat configuration, while the CC2541 was placed in "power mode 1," resulting in a total power consumption of 0.7 mW.

2.7. Measurement and data transmission scenarios for the wireless amperometric circuit

The CC2541 firmware was configured to support calibration, stability and application-specific use-case scenarios. To extract calibration curves, chronoamperometric measurements were performed once every three minutes, with

current levels transmitted every 0.5 seconds for 6seconds. The following 2 minute interval was reserved for sample preparation and incubation. The same scenario was repeated with a 10 minute period for study of the stability of the sensor.

Continuous data transmission with millisecond sampling rates is not required in all application use-cases, and thus the CC2541 firmware was also configured to support duty-cycled measurements. For example, the board was programmed to enable measurement once every few minutes. In this mode, the potentiostat is periodically activated for a period of 60 seconds, or until the current measurement settles. After settling, the current is sampled and transmitted over the wireless link and the concentration is recovered at the receiver based on calibration data. After transmission, the board enters the "sleep mode" for a pre-configured amount of time. Exploiting low-power sleep modes with deeply duty-cycled operation extends the estimated battery life from 12 hours to 5 days.

2.8. Assembly and characterization of integrated wireless mouthguard

After testing the performance of the mouthguard biosensor in artificial saliva and real human saliva, the wireless electronics board was integrated into the mouthguard platform. Stainless steel wires connected to the screen-printed electrode on PET substrate were soldered to the fabricated PCB, and the electronics board together with the printed electrode was assembled into the mouthguard using medical adhesive (Loctite) as shown in Fig. 1A. To test its operation, 100 µl of artificial saliva was placed on the electrode and the same experimental conditions - as described in previous sections (section 2.3) - were applied (supporting video). Chronoamperometric measurements of integrated mouthguard biosensor were carried out by applying -0.3 V (vs. Ag/AgCl) for 1minute following 1 minute of incubation in the sample drop (artificial saliva). The measurement results were sent by Bluetooth wireless data transmission and were displayed on a laptop screen with a custom-made graphical interface. Data communication between the integrated mouthguard sensor and Android smart phones has also been verified using the Texas Instrument BLE Monitor application. For calibration curve extraction, an LED indicator turned on every 3 minutes indicating the time to spike UA to measure the next concentration point. Every time the indicator turned on, a 1 minute long incubation was taken after spiking UA and then the current response was measured for another 1 minute. Stability was also examined in 300 µM UA in artificial saliva at 10 minute intervals

over 4 hours of operation. The sensor was kept in artificial saliva between successive measurements.

3. Results and discussion

3.1. Rationale for salivary uric acid biosensor

Uric acid is the end product of purine metabolism and is excreted by the kidneys and intestinal tract in humans. The normal range of BUA is between 100 and 400 μM (Marshall et al., 2000) and its elevated level is not only an indicator for several renal disorders such as gout, renal disease, hyperuricemia, and Lesch-Nyhan syndrome (Nyhan et al., 1997; Falasca et al., 2006; Nakagawa et al., 2006; Merriman et al., 2011;) but also implies future risk for and increased severity of type 2 diabetes (Costa et al., 2002; Zloczower et al., 2007; Dehghan et al., 2008; Bhole et al., 2010;). It is well-established that there is a high correlation between blood UA level and salivary UA level (Shibasaki et al., 2012; Soukup et al., 2012). Thus, SUA level reflects BUA level so that BUA can be estimated through non-invasive monitoring of SUA. Electrochemical biosensing is the most attractive mode of UA detection due to its advantages such as miniaturization, high sensitivity and cost-effectiveness (Dutt et al., 2005; Chu et al., 2007; Piermarini et al., 2013; Thakur et al., 2013;). Despite these advantages, electrochemical SUA detection has several challenges to overcome. First of all, the electrochemical detection of UA requires high selectivity against ascorbic acid (AA) which is a representative electroactive species in biofluid showing similar oxidation potential. In order to avoid AA interference, uricase enzyme can be utilized to offer selectivity, producing allatonin and hydrogen peroxide (Erden et al., 2013; Piermarini et al., 2013; Thakur et al., 2013). Hydrogen peroxide can be electrochemically measured to determine UA level by either oxidation or reduction. This chemical reaction is described in Fig. 1B. Due to a large over-potential in the oxidation reaction of hydrogen peroxide, other electroactive species in saliva can interfere with the signal through their own oxidation. Therefore, reduction of hydrogen peroxide is preferred and a catalytic mediator is commonly used to lower working potential such as Prussian-blue (Ricci et al., 2005). Saliva is a complex matrix due to its high viscosity (contributes less mass transfer), high protein concentration (induces passivation of electrode under applied potential), and electroactive species (cause interference via oxidation). Therefore, modification of the electrode is highly desired for direct electrochemical measurement of saliva,

especially when monitoring continuously. In a previous paper, our group demonstrated continuous monitoring of salivary lactate for 2hours with electropolymerized o-phenylenediamine (PPD) (Malitesta et al., 1990). The PPD membrane is well known for its capability to reject electroactive species and prevent bio-fouling on an electrode during amperometric measurement. Also, a Prussian-blue transducer offers selective cathodic detection of the hydrogen peroxide produced by the enzymatic reaction of analyte (Ricci et al., 2005). In our current study, a PPD membrane and PB transducer are employed for salivary UA detection in undiluted human saliva. Uricase enzyme was immobilized by cross-linking with BSA and glutaraldehyde, as illustrated in Fig. 1B. This method enabled the biosensor to obtain higher selectivity and sensitivity to the lower physiological level of UA. The resulting BSA-glutaraldehyde-uricase/PPD modified electrode was evaluated through testing in artificial saliva and real undiluted saliva.

3.2 Determination of uric acid with mouthguard sensor in artificial saliva

First, the electrochemical performance of the UA biosensor was evaluated in artificial saliva. A normal SUA level for a healthy person ranges from 100 μM to 250 μM (Shibaski et al., 2012; Soukup et al., 2012). In order to cover a hyperuricemia patient's UA level for diagnostic and treatment applications, a dynamic concentration range of 0-1 mM UA was examined in current response while a potential of -0.3 V(vs. Ag/AgCl) was applied. Fig. 2A displays chronomamperograms for increasing concentrations of UA in 50 μM increments (b–u) in artificial saliva. The data indicates that the PB-PPD-Uricase mouthguard biosensor is very sensitive to UA and has a wide linear range, yielding well-defined chronoamperograms. The corresponding current response is proportional to UA concentration, resulting in the linear calibration plot displayed in the inset of Fig. 2A (Slope, 2.32 μA/mM; correlation coefficient, R^2=0.998).

Since human saliva is a very complex matrix containing various interferents, selectivity should be ensured for real applications. The selectivity was evaluated by continuous measurement under fixed-potential and stirring conditions, in the presence of the relevant species of human saliva, including glucose, lactate, ascorbic acid, and acetaminophen (Mäkilä et al., 1969; Abikshyeet et al., 2012; Smith et al., 1991; Chicharro et al., 1998). As shown in Fig. 2B, the new biosensor displays a favorable response to 350 μM UA, along with a negligible response to other potential

interfering species. Next, a stability test was carried out by measuring the response to 350 µM UA over a 2 hours period at 10 minute intervals, confirming the feasibility of continuous monitoring. Fig. 2C illustrates that the corresponding chronoamperograms are highly stable, with no apparent change throughout this prolonged operation (relative standard deviation (RSD): 3.5%). This stable response indicates efficient enzyme immobilization due to the cross-linking reaction between BSA and glutaraldehyde, as well as the electropolymerized PPD layer.

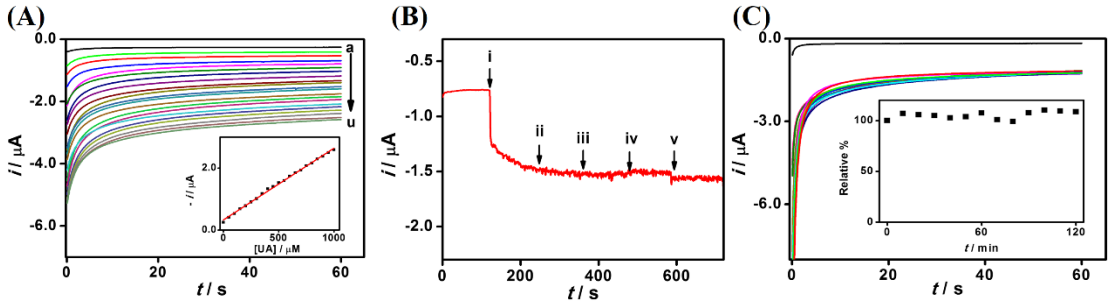

Fig. 2. Electrochemical performance in artificial saliva (A) Chronoamperograms obtained for increasing UA concentration with 50 µM increments up to 1 mM (a-u). The resulting calibration curve is shown in the inset. (B) Selectivity test: response to 350 µM UA (i) in the presence of common electroactive physiological interferents (200 µM AA (ii), 800 µM glucose (iii), 1000 µM LA (iv), and 100 µM ACT (v). (C) Stability of the electrochemical response to 350 µM UA during a 2 h operation with measurements at 10 min intervals. The inset shows the relative current, based on original current response (t=0 s). The sensor kept in artificial saliva between such successive measurements. All experiments were performed with E_{app}=-0.3 V (vs. Ag/AgCl) and a current sampling time of 60 s.

3.3. Determination of uric acid with mouthguard sensor in undiluted human saliva

Next, the performance of biosensor was tested in undiluted human saliva via standard addition method (described in section 2.4). As illustrated in Fig. 3A, the biosensor offers a favorable response to different concentrations of UA in undiluted human saliva, displaying well-defined chronoamperomgrams. The resulting calibration plot, shown in the inset of Fig. 3A, exhibits good sensitivity and linearity (slope, 1.08 µA/mM; correlation coefficient, R^2=0.999). Based on this plot, the SUA level can be estimated to be 488 µM. Despite the presence of numerous potential

interferences in the saliva matrix, e.g., coexisting electroactive materials and proteins, the system offers a well-defined and distinguishable current response within the physiological levels of SUA.

The sensor stability was evaluated in human saliva at 20 minute intervals over 2 hours in order to confirm the absence of biofouling from saliva proteins. The response to SUA after 2 hours shown in Fig. 3B indicates that the developed sensor holds promise for continuous monitoring of the wearer's status. Furthermore, the good linearity and stability of the response (RSD: 4.9 %) provide evidence that the system is applicable in real-life monitoring applications for acute gout, diabetes, and exercise induced oxidative stress.

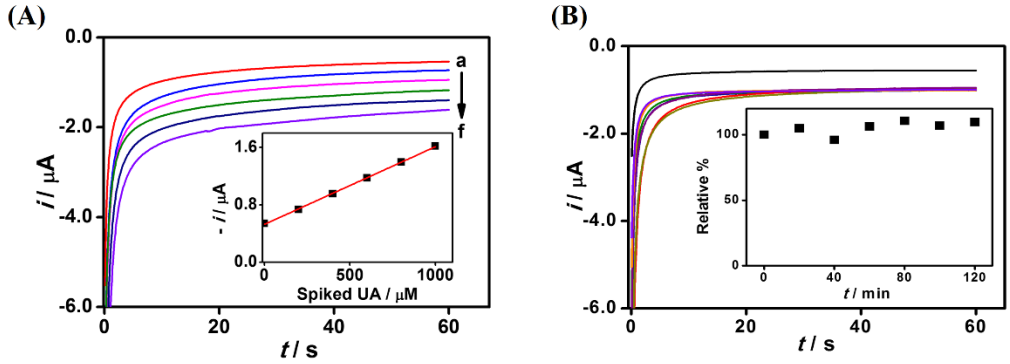

Fig. 3. Electrochemical performance in undiluted human saliva. Chronoamperometric response for undiluted human saliva spiked with increasing concentrations of UA in 0.2 mM increments (a–f). The resulting calibration plot is shown in the inset. (B) Stability of the response in human saliva sample spiked with 350 µM UA. Repetitive measurements were carried out at 20 min intervals over a 2 h period. The inset is the relative current based on original current response (t=0 s). The sensor kept in saliva between such successive measurements. E_{APP}=-0.3 V vs Ag/AgCl and t=60 s.

3.4. Monitoring treatment of hyperuricemia with Allopurinol®

As described in the previous sections, UA monitoring can be applied in a variety of fields, especially in health-care and clinical applications including the diagnosis and treatment of disease. The new mouthguard UA biosensor was tested for practical use in one such application - the monitoring of hyperuricemia. In this study, SUA was monitored and compared using collected saliva from a healthy volunteer and a hyperuricemia patient who was already diagnosed by a physician as having an

elevated BUA level. Fig. 4A displays the SUA level monitored for both the control volunteer and hyperuricemia patient every hour for 5 hours. The SUA level was estimated via standard addition method, similar to the one described in the previous section. Both subjects show consistent SUA levels with small variations–these variations are due to the fact that SUA can be influenced by circadian rhythm during the day and by food intake. Despite of these small variations, there was a significant difference in the measured SUA levels between the healthy volunteer and the hyperuricemia patient (178.5 µM (±20.7 µM) and 822.6 µM (±26.25 µM), respectively). These data support the suitability of the mouthguard sensor as a non-invasive diagnostic tool for hyperuricemia.

The untreated hyperuricemia patient in our test showed a sustained high SUA level for 5 hours - medical action was required to bring these levels to the normal SUA range. The monitoring of this treatment of hyperuricemia under medication is demonstrated in Fig. 4B. The patient in this test was prescribed Allopurinol® to control UA level, which inhibits the activity of Xanthine oxidase and, thus, the production of UA. The patient administered Allopurinol® for 4 days in a row following prescription and the UA concentration in saliva was measured by our sensor 3 times per day to monitor SUA level. This drug helps to control the UA level over the span of days through occasional use. As shown in Fig. 4B, a high level of salivary UA of 816.4 µM (±10.5 µM), out of the normal range, was measured on day zero. Afterwards, during medication, the SUA levels decreased day by day approaching to the normal level within 4 days, reflecting Allopurinol®'s claim. This study proves that the developed mouthguard SUA biosensor can be used for monitoring the treatment of hyperuricemia. This also implies that our biosensor can be applied to monitor the treatment of acute gout, which requires a fast and accurate determination of the treatment's effect, as well as continuous UA monitoring for diabetic patients and athletes.

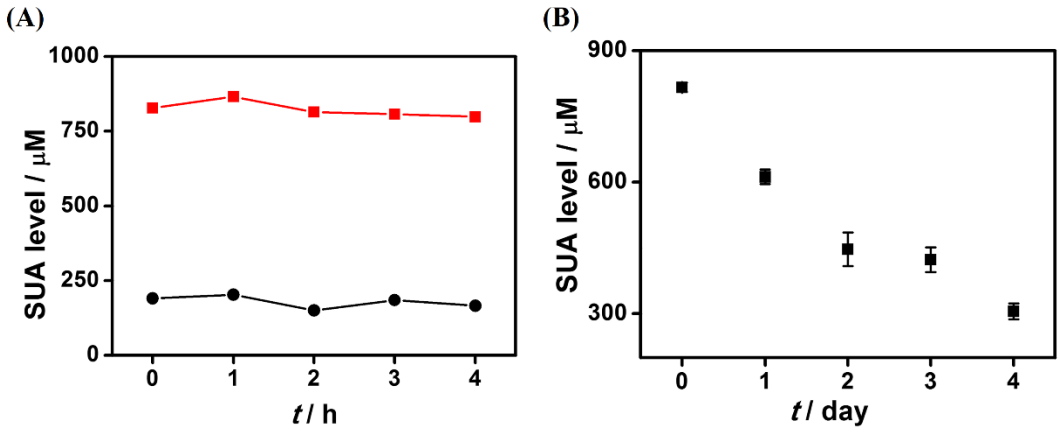

Fig. 4. (A) Monitoring of salivary UA level of healthy volunteer (•) and a hyperuricemia patient (▪) obtained with the mouthguard biosensor over a 5 hour period. (B) Monitoring of SUA level over 5 days of hyperuricemia treatment with Allopurinol®. The result is obtained by average of 3 measurements for each data point.

3.5. Characterization of integrated wireless mouthguard biosensor

The implementation of wearable biosensors for real-time monitoring of saliva has been hindered by the lack of low power far-field wireless transmission circuits. To realize a wearable sensor, a miniaturized Bluetooth-enabled amperometric circuit board was implemented and integrated into a mouthguard biosensor (as shown in Fig. 1A) and its performance was evaluated in artificial saliva in terms of sensitivity and stability. Following the optimized experimental conditions determined with a lab-scale potentiostat, the custom-made board was set to apply the detection potential of -0.3 V for 60 seconds for each measurement. The current response was sampled every 0.5 seconds (a frequency of 2 Hz) and transmitted in real time via Bluetooth 4.0 to a laptop or desktop screen with graphical interface, shown in Fig. 5. Fig. 6A displays the resulting calibration plot for UA detection in artificial saliva obtained by wireless transmission for different UA concentrations up to 600 µM with 100 µM increments, covering possible physiological levels of SUA. The resulting calibration (shown in the inset is highly linear (correlation coefficient R^2=0.998) with a sensitivity of 2.45 µA/mM). The plot produced through wireless transmission shows agreement with the data obtained using a lab-scale potentiostat (CHI), as shown in Fig. 2A.

The stability of our integrated mouthguard biosensor was tested for continuous monitoring applications. As shown in Fig. 6B, the sensor retains its current signal throughout the entire 4 hours of operation with measurements carried out at 10 minute intervals (RSD: 3.13 %). This test provides evidence for the practicality of the wireless wearable mouthguard biosensor towards for relevant health-care monitoring applications.

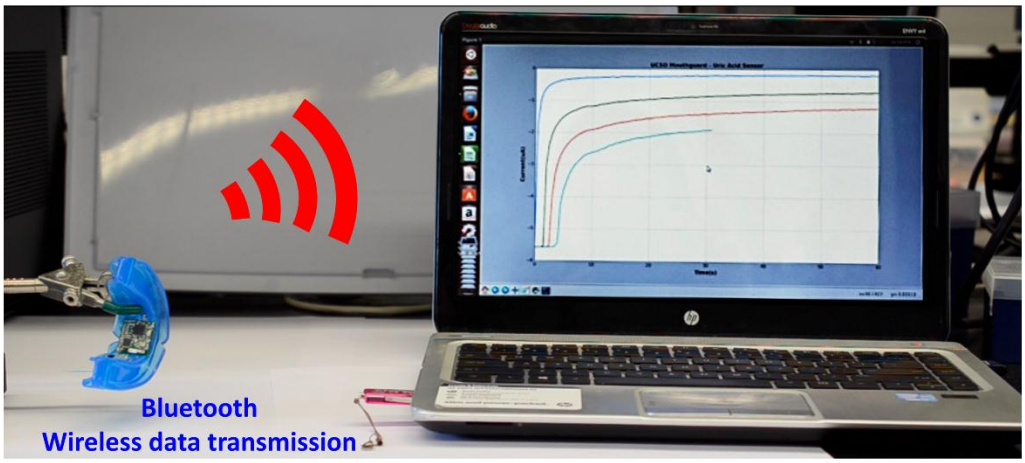

Fig. 5. Real-time monitoring of electrochemical current response of the integrated mouthguard biosensor with wireless data transmission to graphical interface on lap-top via Bluetooth 4.0.

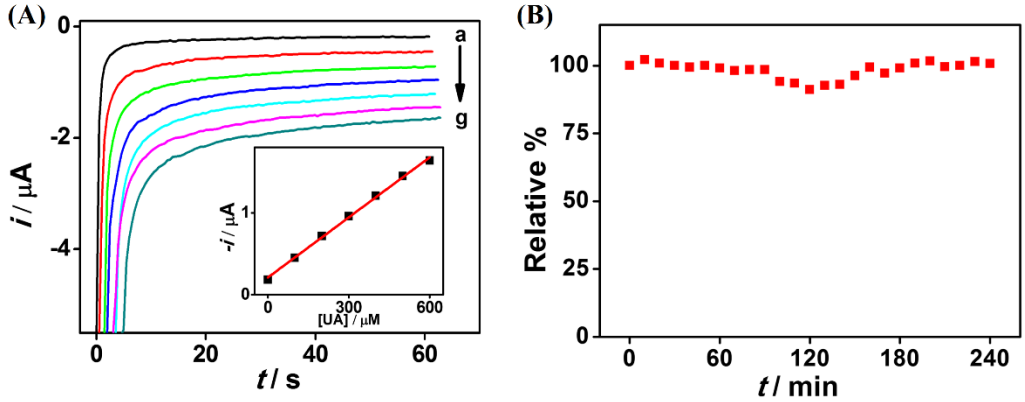

Fig. 6. Electrochemical measurements using the wireless integrated mouthguard biosensor in artificial saliva (A) Chronoamperograms obtained for increasing UA concentration with 100 µM increments up to 600 µM (a-g). The resulting calibration plot is shown in the inset. (B) Stability of the electrochemical response to 300 µM UA during a 4 hour operation with measurements carried out at 10 min intervals.

4. Conclusions

The present work describes an integrated wireless mouthguard amperometric biosensor for real-time monitoring of salivary UA. The new wearable mouthguard biosensor has been coupled with a miniaturized printed circuit board for wireless data collection. The biosensor displays attractive electrochemical performance with high selectivity, sensitivity and stability. Future efforts will focus on a critical assessment of potential toxicity and biocompatibility issues essential for the realization of real-time 'in mouth' testing on humans. The new mouthguard sensor platform can be readily expanded to a multiple salivary analytes in connection to a sensor array, along with further miniaturization of the circuit board and wireless transceiver for diverse fitness and biomedical daily-life applications.

Acknowledgements

This work was supported by the National Institute of Biomedical Imaging and Bioengineering of NIH (under Award Number R21EB019698. US NIH) and by the Air Force Research Laboratory (through the FlexTech Consrtium -LTR SUBK). The views and conclusions contained herein are those of the authors and should not be interpreted as necessarily representing the official policies or endorsements of the National Institutes of Health, Air Force Research Laboratory, or the U.S. Government. W. R. de Araujo and J. Warchall acknowledge financial support from FAPESP-BEPE (2014/00788-0) and an NSF Graduate Research Fellowship (under Grant No. DGE-1144086), respectively.

References

Abikshyeet, P., Ramesh, V., Oza, N., 2012. Diabetes Metab Syndr Obes, 5, 149.
Andreu Perez, J., Leff, D., Ip, H., Yang, G. Z., 2015. IEEE, In press. DOI:10.1109/TBME.2015.2422751

Bandodkar, A. J., Hung, V. W., Jia, W., Valdés-Ramírez, G., Windmiller, J. R., Martinez, A. G., Ramirez, J., Chan, G., Kerman, K., Wang, J., 2013. Analyst, 138, 123-128

Bandodkar, A.J., Wang, J., 2014a. Trends Biotechnol. 32, 363-371.

Bandodkar, A. J., Molinnus, D., Mirza, O., Guinovart, T., Windmiller, J. R., Valdés-Ramírez, G., Andrade, F. J., Schöning, M. J., Wang, J. 2014b, Biosens. Bioelectron. 54, 603-609.

Bandodkar, A. J., Jia, W., Yardımcı, C., Wang, X., Ramirez, J., Wang, J. 2015. Anal. Chem. 87, 394-398.

Bhole, V., Choi, J. W. J., Kim, S. W., De Vera, M., Choi, H., 2010. Am. J. Med. 123, 957-961.

Chicharro, J. L., Lucía, A., Pérez, M., Vaquero, A. F., Ureña, R. 1998. Sports Med. 26, 17-27.

Chu, Q. C., Lin, M., Geng, C. H., Ye, J. N., 2007. Chromatogr. 65, 179-184.

Claver, J. B., Mirón, M. V., Capitán-Vallvey, L. F., 2009. Analyst, 134, 1423-1432.

Corrie, S. R., Coffey, J. W., Islam, J., Markey, K. A., Kendall, M. A. F., 2015. Analyst In press. DOI: 10.1039/C5AN00464K

Costa, A. I. J. L. I., Igual, I., Bedini, J., Quint, L., Conget, I.,2002. Metabolism. 51, 372-375.

Dehghan, A., Van Hoek, M., Sijbrands, E. J., Hofman, A., Witteman, J. C. 2008. Diabetes care, 31, 361-362.

Depari, A., Flammini, A., Rinaldi, S., Vezzoli, A., 2013. Sens. Actuators A: Phys. 202, 147–154.

Diamond, D., Lau, K. T., Brady, S., Cleary, J., 2008. Talanta, 75, 606–612.

Dutt, J. S., Cardosi, M. F., Livingstone, C., Davis, J., 2005. Electroanalysis, 17, 1233-1243.

Endo, H., Yonemori, Y., Hibi, K., Ren, H., Hayashi, T., Tsugawa, W., Sode, K., 2009. Biosens. Bioelectron. 24, 1417–1423.

Erden, P. E., Kılıç, E., 2013. Talanta, 107, 312-323.

Falasca, G.F., 2006. Clini. Dermatol. 24, 498-508.

Ghafar-Zadeh, E., 2015. Sensors, 15, 3236-3261.

Graf, H., Mühlemann, H. R., 1966. Helv. Odontol. Acta 10, 94-101.

Graf, H., Mühlemann, H.R., 1969. Arch. Oral Biol. 14, 259-IN3.

Hellsten, Y., Tullson, P. C., Richter, E. A., Bangsbo, J., 1997. Free Radic. Biol. Med. 22, 169-174.

Hibi, K., Hatanaka, K., Takase, M., Ren, H., Endo, H., 2012. Sensors, 12, 6269–6281.

Humphrey, S. P., Williamson, R. T., 2001. J. Prosthet. Det. 85, 162-169.

Jia, W., Bandodkar, A. J., Valdés-Ramírez, G., Windmiller, J. R., Yang, Z., Ramírez, J., Chan, G., Wang, J., 2013. Anal. Chem. 85, 6553-6560.

Kassal, P., Steinberg, I.M. & Steinberg, M.D., 2013. Sens. Actuators B: Chem. 184, 254–259.

Kassal, P., Kim, J., Kumar, R., de Araujo, W. R., Steinberg I. M., Steinberg M.D., Wang, J., 2015. Electrochem. Commun. 56, 6–10.

Kim, J., Valdés-Ramírez, G., Bandodkar, A. J., Jia, W., Martinez, A. G., Ramírez, J., Mercier, P., Wang, J., 2014. Analyst, 139, 1632-1636.

Kim, J., de Araujo, W. R., Samek, I. A., Bandodkar, A. J., Jia, W., Brunetti, B., Paixão, T. R. L.C., Wang, J., 2015. Electrochem. Commun. 51, 41-45.

Malitesta, C., Palmisano, F., Torsi, L., Zambonin, P. G., 1990. Anal. Chem. 62, 2735-2740.

Mannoor, M. S., Tao, H., Clayton, J. D., Sengupta, A., Kaplan, D. L., Naik, R. R., Verma, N., O,emettp, F. G., McAlpine, M. C., 2012. Nat. Commun. 3, 763.

Mäkilä, E., Kirveskari, P., 1969. Arch. Oral Biol., 14, 1285-1292.

Marshall W. J., Clinical Chemsitry, 4th ed, Mosby, 2000.

Matzeu, G., Florea, L., Diamond, D., 2015. Sens. Actuators B: Chem, 211, 403-418.

Merriman, T. R., Dalbeth, N., 2011. Joint Bone Spine, 78 1, 35-40.

Moran, M. E., Front. Biosci. 2003, 8, S1339.

Nakagawa, T., Hu, H., Zharikov, S., Tuttle, K. R., Short, R. A., Glushakova, O., Ouyang X., Feig D. I., Block E. R., Herrera-Acosta J., Patel J. M., Johnson R. J., 2006. Am. J. Physiol. Renal Physiol. 290, F625-F631.

Navazesh, M., 1993. Annals of the New York Academy of Sciences 694.1, 72-77.

Nyhan, W. L., 1997. J. Inherit. Metab. Dis. 20, 171-178.

Owen-Smith, B., Quiney, J., Read, J. 1998. The Lancet, 351, 1932.

Piermarini, S., Migliorelli, D., Volpe, G., Massoud, R., Pierantozzi, A., Cortese, C., Palleschi, G., 2013. Sens. Actuators B: Chem. 179, 170-174.

Ricci, F., G. Palleschi. 2005. Biosens. Bioelectron. 21, 389-407.

Shibasaki, K., Kimura, M., Ikarashi, R., Yamaguchi, A., Watanabe, T., 2012. Metabolomics, 8, 484-491.

Smith, M., Whitehead, E., O'Sullivan, G., Reynolds, F., 1991. Br. J. Clin. Pharmac., 31, 553-555.

Soh, P. J., Vandenbosch, G., Mercuri, M., Schreurs, D. M. P., 2015. IEEE Microw. Mag., 16, 55-70.

Soukup, M., Biesiada, I., Henderson, A., Idowu, B., Rodeback, D., Ridpath, L., Bridges, K. G., 2012. Diab. Metab. Synd. 4, 14.

Thomas, N., Lähdesmäki, I., Parviz, B. A. 2012. Sens. Actuators B: Chem. 162, 128-134.

Thakur, B., Sawant, S. N., 2013. ChemPlusChem, 78, 166-174.

Windmiller, J. R., Wang J., 2013. Electroanalysis 25, 29-46.

Yao, H., Liao, Y., Lingley, A. R., Afanasiev, A., Lähdesmäki, I., Otis, B. P., Parviz, B. A., 2012. J. Micromech. Microeng. 22, 075007.

Zhang, D., Jing, J., Junye, C., Qian, Z., Yanli, L., Yao, Y., Shuang, Li., Gang, L. L., Qingjun, L., 2015. Biosens. Bioelectron. 70, 81–88.

Zloczower, M., Reznick, A. Z., Zouby, R. O., Nagler, R. M., 2007. Antioxid. Redox Signal. 9, 765-773.

Zuliani, C., Matzeu, G., Diamond, D., 2014. Electrochim. Acta 132, 292-296.